How to make fragile bonds no longer fragile towards electrons for robust organic optoelectronic materials

Rui Wang[1], Qing-Yu Meng[1], Yi-Lei Wang[1], and Juan Qiao[1,2]*

[1]Key Lab of Organic Optoelectronics and Molecular Engineering of Ministry of Education, Department of Chemistry, Tsinghua University, Beijing 100084, P. R. China

[2]Center for Flexible Electronics Technology, Tsinghua University, Beijing 100084, P. R. China

*E-mail: qjuan@mail.tsinghua.edu.cn.

ABSTRACT The development of robust organic (opto)electronic devices is mainly hindered by the chemical deterioration of organic materials on service. For organic light-emitting diode (OLED) materials, a key molecular parameter for intrinsic chemical stability is the bond-dissociation energy of the fragile bond (BDE_f) with the lowest BDE in the molecule. Although rarely concerned, most OLED molecules have the lowest BDE_f in negatively charged states ($BDE_f(-)$, ~1.6−2.5 eV), which would be a fatal short-slab for device stability. Here, we confirmed the close correlation between $BDE_f(-)$, intrinsic material stability, and device lifetime. To make fragile bonds no longer fragile towards electrons, we found that introducing strong electron-withdrawing groups with delocalizing structures would be an effective and universal strategy, which was found in typical phosphine-oxide and carbazole module molecules and backed by comparisons in several reported and newly designed molecules. It not only substantially improves $BDE_f(-)$ by ~1 eV, but revives the originally vulnerable building blocks, thus largely enriches available groups for rational design of robust OLED and other organic (opto)electronic materials.

Introduction

The operational stability is a crucial and common issue for organic (opto)electronic devices.[1–4] In particular, it is one of the greatest remaining problems for the popular organic light-emitting diodes (OLEDs). The intrinsic degradation of OLEDs is mainly ascribed to the chemical deterioration of organic (or metal-organic) materials.[4–9] Many undesired (photo)physical processes could induce such chemical deterioration, like exciton−polaron and exciton−exciton annihilations (EPA and EEA), in which EPA has been confirmed as a dominate mechanism.[10–16] In this process (Fig. 1a), one exciton transfers energy to a polaron, generating an excited (*hot*) polaron whose energy could be high enough to break chemical bonds, the products could act as exciton quenchers, charge traps, and nonradiative recombination centers. In past decades, considerable efforts have been made to suppress the undesired (photo)physical processes.[11,12,18–23] However, completely avoiding them at the microscopic level is scarcely possible, while a small amount of deterioration products can result in 50% luminance loss.[10,24] To date, lifetime of efficient blue OLEDs (exciton energy usually ≥ 2.7 eV) still cannot satisfy practical applications. Therefore, restraining the induced (photo)chemical deteriorations is essential.

According to thermodynamics, the bond most probable to break would be the fragile bond with the minimum (or comparable-to-the-minimum) bond-dissociation energy (BDE) in a molecule. Its BDE (BDE_f) is confirmed as a key parameter for the intrinsic stability of OLED materials.[24–33] Generally, chemical bonds of organic molecules are particularly vulnerable in negatively charged states. In Fig. 1b and 1c, we compared $BDE_f(n)$, $BDE_f(+)$, and $BDE_f(-)$ (*n*, +, and − refer to neutral, positively and negatively charged states) of typical fragile exocyclic C−X single bonds (X = heteroatoms like N, P, S, etc.) in several representative OLED molecules. It can be found their $BDE_f(n)$ and $BDE_f(+)$ are 3.1−4.8 eV, while most $BDE_f(-)$ are

only 1.6−2.5 eV. Many OLED molecules have comparable $BDE_f(-)$ values.[6,27,28,33,34] As a result, once such negatively polaron are generated and/or get involved in EPA, the fragile bond would inevitably dissociate and incur chemical degradation. Thus, $BDE_f(-)$ would be a fatal short-slab for intrinsic material stability for OLED materials.

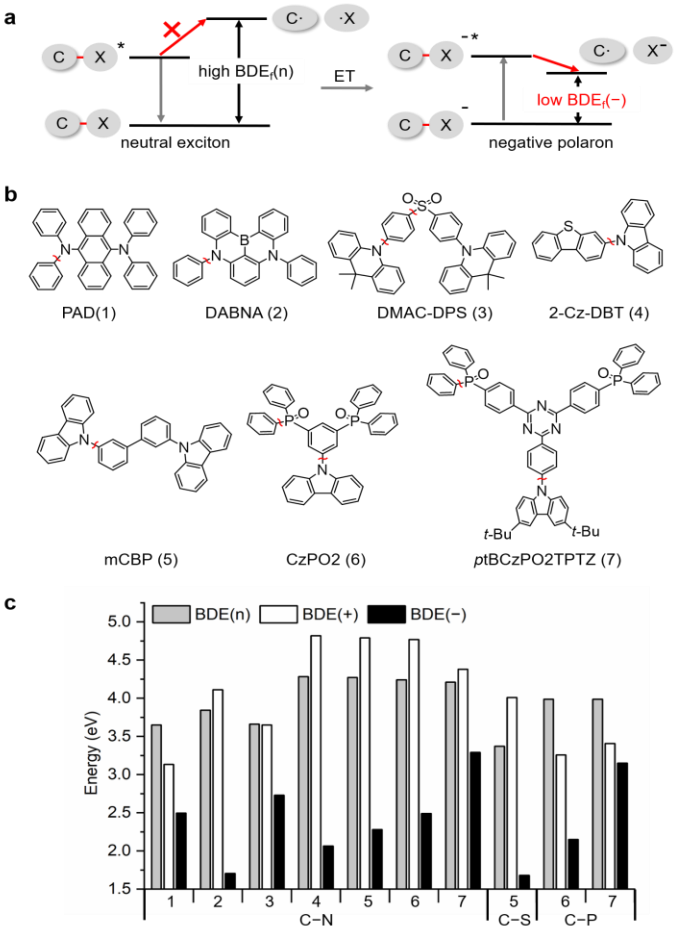

Figure 1 | $BDE_f(-)$ issue of OLED molecules. a, Schematic of the potential mechanism of EPA-induced bond-dissociation of the negative polaron. The asterisk refers to the excited state. $BDE_f(n)$ and $BDE_f(-)$ refers to the bond-dissociation energies of the fragile C−X bonds under neutral and negatively charged states, respectively. ET refers to energy transfer. **b,** Chemical structures of typical OLED molecules **1**−**7**. The fragile bonds are highlighted by the red markers. **c,** BDE_f values of the interested molecules. Calculations were at the M06-2X/def2-SVP level.

However, studies on regulating $BDE_f(-)$ values of OLED molecules are scarce.[28,33,34] Other researches on BDE(−) of organics are mainly about organic halides.[35–37] Different from $BDE_f(n)$ which mainly depends on the bond type, as evidenced by the almost identical $BDE_f(n)$ values of the same C−N (from carbazole, Cz) or C−P (from phosphine-oxide, PO) bonds in **4**−**7**, $BDE_f(-)$ is largely affected by molecular structures (Fig. 1d). Considering that Cz is almost the most common building block in OLED molecules,[6–9] PO-based hosts and other materials are one of the most popular in OLEDs,[38–43] Cz and PO derivatives are representative and meaningful instances for studying $BDE_f(-)$. Notably, there is an accepted cognition that PO could undermine the device stability due to the fragile C−P bond.[6,27,28,38] For instance, CzPO2 whose $BDE_f(-)$ is only 2.15 eV (Fig. 1c) did show serious C−P bond cleavage in laser-desorption/ionization time-of-flight mass spectrometry (LDI-TOF-MS) and electrical-stress tests. However, $BDE_f(-)$ of the same C−P bond in *p*tBCZPO2TPTZ is as high as 3.15 eV, therefore it did not show observable deterioration in LDI-TOF-MS until very high laser powers, suggesting its C−P bonds are relatively stable (Supplementary Fig. S1 in Supporting Information). This result enlightened us that the original fragile bonds can be turned

into stable ones, and it drove us to dissect general relationship between molecular structures and $BDE_f(-)$, which will make an essential contribution to improving the operational stability of OLEDs and other organic (opto)electronic devices.

Herein, we first conducted quantum chemical (QC) calculations, LDI-TOF-MS tests, electrical stresses on single-carrier devices, and lifetime measurements of OLEDs, revealed how $BDE_f(-)$ affects intrinsic material stability and device lifetime. Second, we took a systematic theoretical study on typical PO and Cz-derivatives, developed an effective and universal strategy to manage $BDE_f(-)$ based on a fundamental thermodynamic equation, which was further validated by the comparisons in several reported and newly designed molecules. Importantly, this strategy can not only improve BDE_f greatly (often by ~1 eV), irrespective of the type of the fragile bond, but revive the originally vulnerable building blocks, thus largely enriching available groups for the development of robust OLED and other organic optoelectronic materials.

Comparative studies on TP3PO and PO-T2T

To isolate the concerned $BDE_f(-)$ from other material-related parameters (e.g. exciton energy and thermal stability), we comparatively studied the intrinsic stability of two representative PO-based electron-transporting materials (ETM), TP3PO and PO-T2T, with very similar chemical structures (Fig. 2a).[42,43] The structural similarity leads to similar molecular parameters (Supplementary Fig. S2 and Table S1). As for molecular stability, $BDE_f(n)$ values in TP3PO and PO-T2T are all close to 4.00 eV for the C−P bonds (details are in Supplementary Table S2−S3), while their $BDE_f(-)$ values show large disparity, as low as 2.49 and 2.78 eV for C1−P and C2−P bonds of TP3PO, but as high as 3.43 and 3.60 eV for those of PO-T2T. The low $BDE_f(-)$ of TP3PO would cause undesired chemical degradations, while the high $BDE_f(-)$ of PO-T2T is enough to afford exciton energies in most OLEDs, which may disburden this material of undesired degradations.

To validate these speculations, we conducted LDI-TOF-MS tests, which have proved be powerful to analyze the degradations of OLED materials.[4,24,27,28,31] Here, samples were pure powder of TP3PO and PO-T2T. Under the negative detection mode, the laser intensity was set to increase gradually from 90 to 110 μJ/pulse to track the degradation process (all spectra are in Supplementary Fig. S3). At the lowest intensity of 90 μJ/pulse, TP3PO showed weak molecular and quasi-molecular ion peaks ($[M \pm H]^-$, etc.), and C2−P bond cleavage peaks $[M - POPh_2]^-$; but very strong C1−P bond cleavage peaks $[M - Ph]^-$ and $[M[O] - Ph]^-$. As the laser intensity increased, the $[M \pm H]^-$ and $[M - POPh_2]^-$ almost disappeared, while the $[M - Ph]^-$ and $[M[O] - Ph]^-$ became very conspicuous. In comparison, at 90 μJ/pulse, PO-T2T showed strong $[M \pm H]^-$, but very weak $[M - Ph]^-$ and $[M[O] - Ph]^-$. It is not until the intensity exceeded 100 μJ/pulse that the $[M - Ph]^-$ and $[M[O] - Ph]^-$ became stronger than the $[M \pm H]^-$. The $[M - POPh_2]^-$ of PO-T2T was very weak throughout the entire process.

The LDI-TOF-MS results accord well with BDE predictions. Specifically, (i) For both TP3PO and PO-T2T, C1−P bonds with lower BDE are more fragile than C2−P bonds. (ii) TP3PO showed remarkable C1−P bond cleavage peaks sooner than PO-T2T with the increasing laser intensity, manifesting its poorer material stability. Therefore, LDI-TOF-MS results strongly support that BDE_f is a key molecular parameter for the intrinsic material stability. Since QC-calculations and experiments both suggest that C1−P (C1 means the unsubstituted phenyl) are more fragile than C2−P bonds, the following studies on PO-derivatives mainly focus on C1−P bonds.

Device degradation experiments

To correlate material stability with device stability, we first fabricated TP3PO- and PO-T2T-based electron-only devices (EODs), with the structure ITO|PO-T2T (120 − x nm)|TP3PO (x nm)|TPBi (20 nm)|LiF (1 nm)|Al (120 nm) (Fig. 2b). Under the electrical stress (10 mA cm^{-2}), we found that the aging of the EODs become more rapid as the thickness of TP3PO increases. For x = 0, 5, 20, and 120, the voltage increases (ΔV) of the EODs after 5 h stress are 0.04, 1.57, 4.41, and 20.52 V, respectively

(Fig. 2c). This result clearly demonstrates that the instability of TP3PO anion is the main cause of the voltage rise. Next, we fabricated OLEDs with the structure ITO|HATCN (10 nm)|NPB (30 nm)|TCTA (15 nm)|mCBP (15 nm)|DPEPO:30 wt% TCzTrz|PO-T2T (40 − *x* nm)|TP3PO (*x* nm)|TPBi (5 nm)|LiF (1 nm)|Al (120 nm) (*x* = 5, 10, 30, or 35; Fig. 2d). TCzTrz is a sky-blue emitter developed by Zhang *et al.*[44] All these OLEDs demonstrated close (~11%) maximum efficiencies (Supplementary Fig. S5), which are comparable to reported values.[44] Fig. 2e shows their half-life (LT50) when operating at an initial brightness of 500 cd m^{-2}. For the devices *x* = 5, 10, 30, and 35, LT50 values are 12.0, 11.0, 7.7, and 4.2 h, respectively. Since the only difference between these devices is the thicknesses of TP3PO and PO-T2T, the result further supports that it is the TP3PO with much lower $BDE_f(-)$ that accounts for device degradations.

To rationally link macroscopic devices degradation with microscopic bond cleavage, we further calculated energy levels of PO-containing anions resulted from the bond cleavage of TP3PO and PO-T2T. Supplementary Fig. S6 shows that HOMO of PO-containing anions (−1.72 to −2.20 eV) are much lower than LUMO (−0.79 to −1.27 eV) of the intact molecules. Hence, once generated, these anions would act as filled-deep traps, hindering the transport and injection of other negative charges. Since TP3PO is more fragile towards electrons, the corresponding device would generate much more defects in the same time scale, thus showing poorer operational stability.

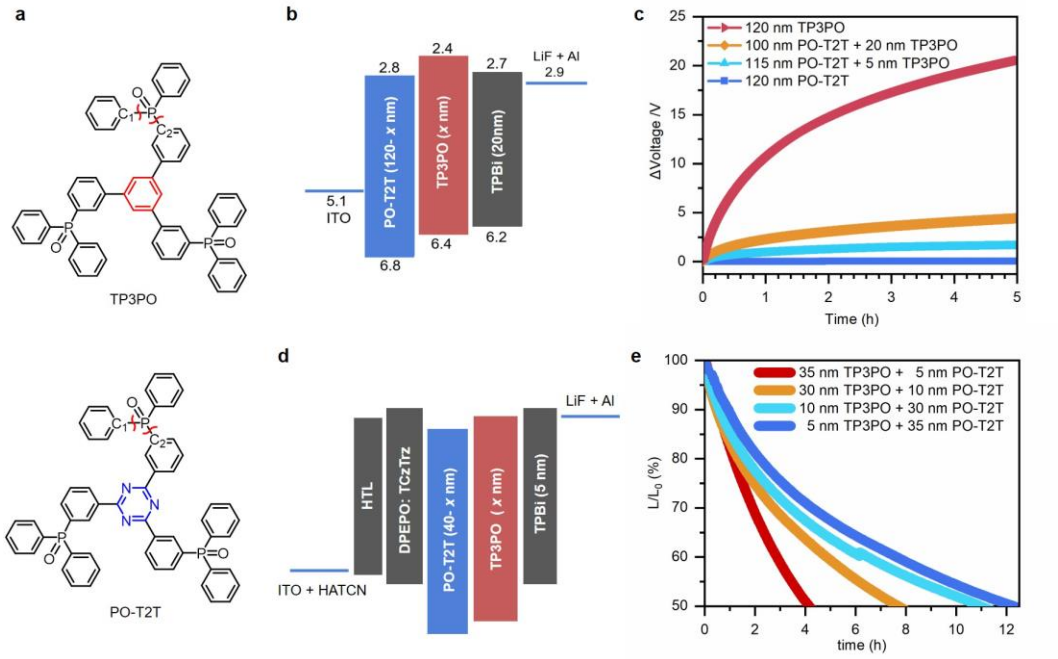

Figure 2 | Comparative study of TP3PO and PO-T2T. a, Chemical structures of TP3PO and PO-T2T, the fragile bonds are highlighted by the red markers. **b,** Device structures of the EODs (*x* = 0, 5, 20, or 120). The current density-voltage curves of the devices are in Supplementary Fig. S4. **c,** Change of the voltages of EODs during 5 h under a constant current density of 10 mA cm^{-2}. **d,** Device structures of the OLEDs (*x* = 5, 10, 30, or 35). Chemical structures of the involved organic materials are shown in Supplementary Fig. S5. To prevent the introduction of new interfaces, devices with solely TP3PO (or PO-T2T) as the ETM were not fabricated. **e,** The operation lifetime of the OLEDs measured at a brightness of 500 cd m^{-2} under a constant current.

Up to here, we comprehensively demonstrated the close correlation between $BDE_f(-)$, intrinsic material stability, and device lifetime, and revealed that active organic materials with lower $BDE_f(-)$ would result in poorer material stability and device lifetime. It is noteworthy that the comparison between TP3PO and PO-T2T demonstrates that with appropriate molecular design, the original vulnerable groups can serve in robust materials. Therefore, it would be imminent to reveal the relationship between $BDE_f(-)$ and molecular structure, and establish feasible design strategies to improve $BDE_f(-)$.

Key influence factors of $BDE_f(-)$

For the C−X (X = N, P, S, etc.) bonds in OLED molecules, X-sides usually have higher electronegativities, so the bond dissociations in negative charged molecules will result in anions containing X. According to the Hess's law, an equation between $BDE_f(-)$ and $BDE_f(n)$ can be derived (Scheme 1),

$$BDE_f(-) = BDE_f(n) + EA_M - EA_X \quad (1)$$

where EA_X and EA_M represent the electron affinity of the X radical and the intact molecule, respectively. For all C−X bonds in Fig. 1b, it is their EA_X values (2−2.6 eV) significantly higher than EA_M values (0.3−1.5 eV) that lead to largely reduced $BDE_f(-)$. Most importantly, the equation suggests how to control $BDE_f(-)$. For $BDE_f(n)$, it mainly depends on the type of C−X bond and rarely influenced by other parts of the molecule except *ortho*-substituents.[26,34] Although *ortho*-substituents may cause large influences (up to 0.5 eV), the effects depend on case-specific spatial factors and electronic characters of the substituents.[26] So these distinct effects are not involved here. For EA_M, it can be ideally increased by introducing electron-withdrawing groups (EWGs) on C-side of C−X bond. It is feasible when X is an atom (e.g. halogen). However, in OLED molecules, X-sides are usually building blocks and the substitutions are ubiquitous. Moreover, many OLED molecules have several C−X bonds (Fig. 1b), modifications on the C-side of one C−X bond may be right on the X-sides of the others. In these cases, introducing EWGs would lead to simultaneous increase of EA_M and EA_X, which may result in a limited increase or even decrease of $BDE_f(-)$. The question then arises: to obtain a high $BDE_f(-)$, how to improve EA_M accurately without increasing EA_X as much as possible? To address this, an in-depth study between EA_M, EA_X and molecular structure is indispensable.

Scheme 1. Derivation of the calculation formula of $BDE_f(-)$.

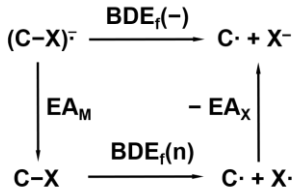

Improving $BDE_f(-)$ values of PO-derivatives

We first looked into the parent molecule $POPh_3$. Fig. 3a shows the negative charge in $POPh_3$ anion mainly distributes on the LUMO, while that of the $POPh_2$ fragment anion is mainly on sp^3-orbital of P. Thus, EA_M and EA_X are basically determined by the distinct orbitals. To increase EA_M, introducing strong EWGs and/or delocalizing structures are two typical ways. Meanwhile, they would have smaller impact on EA_X due to the localization of sp^3-orbital. Accordingly, we designed **P2**−**P4** with strong EWGs introduced to $POPh_3$ (**P1**), including trifluoromethyl (**P2**), cyano (**P3**), or replace one of the phenyl with 1,3,5-triazine (**P4**); and **P5**−**P6** with relatively weaker EWGs but delocalizing structures, including pyridine (**P5)** and 5'-phenyl-[1,1':3',1"-terphenyl]-4-yl (PTP) (**P6**) (Fig. 3b). Calculations show that EA_M values of **P2**−**P6** all increase by 0.6−1 eV, higher than the increase of EA_X values (≤0.45 eV). Of note, EA_X values of **P5**−**P6** are ~0.2 eV smaller than those of **P2**−**P4**. In total, $BDE_f(-)$ values of **P2**−**P6** increase to 2.15−2.55 eV, which are considerably higher than that of **P1** (1.87 eV), yet still comparable to the $BDE_f(-)$ of the unstable TP3PO (2.49 eV). Thus, a greater enhancement is demanded. Incidentally, substituents at *meta*-positions of P atom bring similar effects (Supplementary Table S4).

Since strong EWGs and delocalizing structures can both increase EA_M, and the latter has a smaller influence on EA_X, we thus combined the two methods into a more effective strategy, namely introducing strong EWGs with delocalizing structures (D-EWGs), and designed **P7** and **P8**. Really, introductions of benzonitrile in **P7** and 4-(4,6-diphenyl-1,3,5-triazin-2-yl)phenyl

(Trz) in **P8** remarkably increase EA_M by over 1.2 eV, which do outperform the effect of solely introducing of EWGs or delocalizing structures. We found the contribution of the $POPh_2$ moiety to LUMO is only 8.7% in **P8**, considerably smaller than those in **P4** (24.7%) and **P6** (12.2%), indicating that D-EWGs effectively confine the negative charge. Moreover, D-EWGs could suppress the increase of EA_X. For instance, **P3** and **P7** both have a cyano; while **P7** has an increased distance between the cyano and P atom, thus leading to a smaller EA_X increase (0.32 *vs* 0.45 eV for **P7** and **P3**). Consequently, D-EWGs significantly improve $BDE_f(-)$ values of **P7** and **P8** to 2.73 and 3.04 eV (Fig. 3b). Such values are high enough to afford the exciton energies in many OLEDs. Notably, the ability of stabilizing the negative charge is the inherent character of D-EWGs; meanwhile, they often increase the distance to X. Therefore, introducing D-EWGs could be a universal strategy for improving $BDE_f(-)$. For aryl amide and sulfone derivatives, D-EWGs likewise increase their $BDE_f(-)$ values by ~1 eV (Supplementary Table S5).

Importantly, D-EWGs not only improve the thermodynamic stability reflected by BDE_f, but suppress the kinetic process of bond cleavages. That is confirmed by the comparison between the rapid degradation of TP3PO-only EOD, and the robustness of PO-T2T-only EOD. During C−P bond cleavages towards electrons, the electron on LUMO redistributes to sp^3-orbital of P.

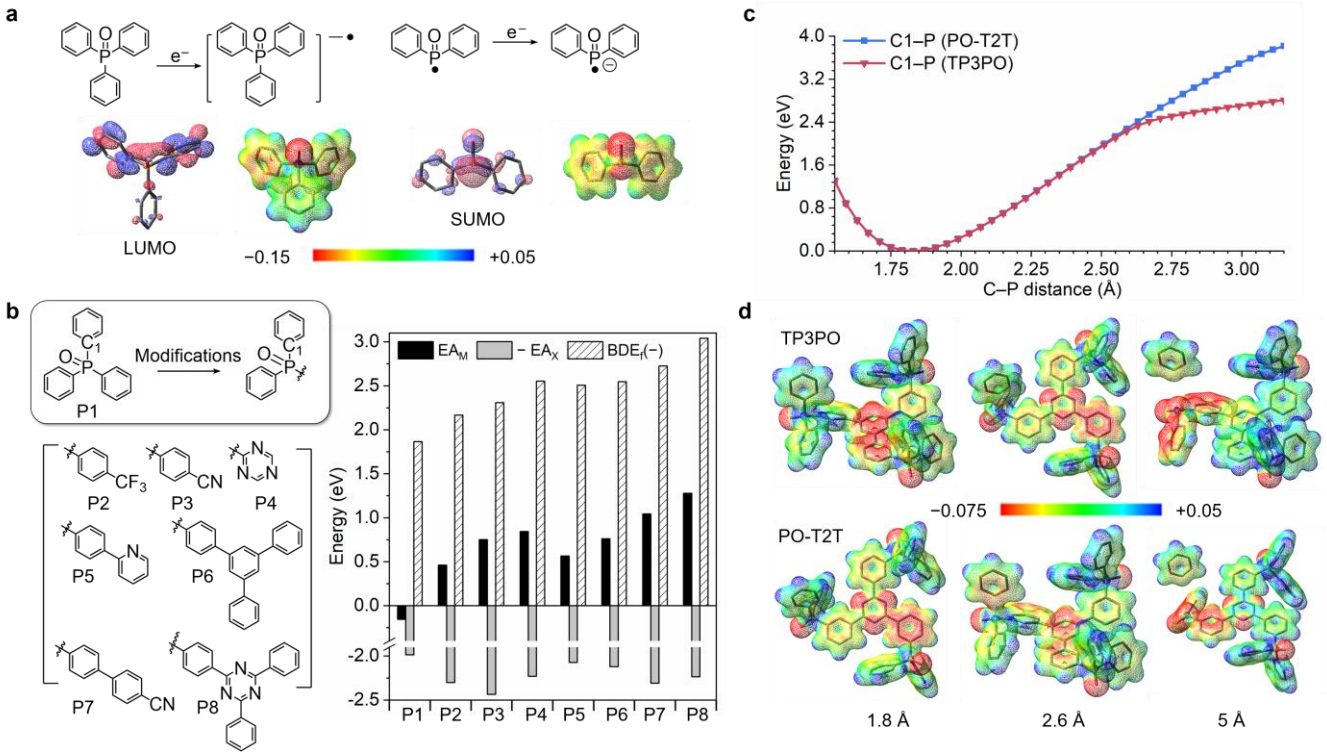

Figure 3 | Study on improving $BDE_f(-)$ values of PO-derivatives**. a,** Frontier orbital (isovalue = 0.03 au) and ESP maps of $POPh_3$ and $POPh_2$. **b,** Chemical structures, EA_M, EA_x, and and $BDE_f(-)$ values (with respect to C1−P bond) of molecules **P1**−**P8**. **c,** Potential energy curves with respect to the stretch of C1−P bonds (1.55−3.15 Å) in TP3PO and PO-T2T anions. **d,** ESP maps (isovalue = 0.02 au) when the C1−P distance is 1.8, 2.6, and 5 Å, respectively. All calculations were at the M06-2X/def2-SVP level.

When there are D-EWGs that confine the negative charge, the redistribution will become more difficult. To visualize this, potential energy curves (PECs) and electrostatic potential (ESP) maps are plotted during C1−P bond cleavages in TP3PO and PO-T2T anions. Fig. 3c shows that PECs of the two anions are almost identical when C−P distance is ~1.8 Å. However, when the distance is over 2.6 Å, PECs of PO-T2T clearly increase faster than those of TP3PO. In ESP maps (Fig. 3d), when C1−P distance is 1.8 Å, the negative ESP (red) is mainly allocated around the center for both molecules (also see Supplementary Fig. S7). While at 2.6 Å, the red color within the central of TP3PO clearly becomes shallower; while that in PO-T2T scarcely changes. From 1.8 Å to 2.6 Å, the negative charge allocated around the central aryl (q_{Ar}) changes from −0.76 to −0.60 for

TP3PO, while in PO-T2T, q_{Ar} only changes from −0.75 to −0.72. Finally, when the phenyl leaves, the negative charge is concentrated around PO, while q_{Ar} of PO-T2T is still higher than that of TP3PO (−0.35 *vs* −0.27, Supplementary Table S6). This clearly reflects that Trz effectively restricts the negative charge. From this perspective, introducing D-EWGs is also a promising strategy to protect C−X bonds and improve their kinetic stability towards electrons in principle. Next, we further demonstrate that the strategy is also effective for Cz-derivatives, even though Cz and PO have quite different electronic structures.

Improving $BDE_f(-)$ values of Cz-derivatives

For Cz-derivatives, substituents on N-side (Cz) or on C-side (Ph) of the C−N bond would have distinct effects on EA_M and EA_X. We first studied the substituent effects on N-side. Based on the parent PhCz (**C1**, Fig. 4a), we introduced the cyano, PTP, and Trz groups into 2- and 3-sites of Cz, respectively. At 3-site, cyano dramatically increases EA_X by 0.63 eV, due to its strong interaction with the delocalized SUMO of Cz radical (Supplementary Fig. S8).[34] Such increase is even higher than that of EA_M (0.5 eV, Fig. 4b), resulting in a decreased $BDE_f(-)$ (1.39 vs 1.45 eV for **C2** and **C1**). In comparison, PTP brings much smaller increase of EA_X (0.25 eV), but bigger increase of EA_M (0.7 eV), thus leading to a higher $BDE_f(-)$ (1.89 eV) for **C3**. Likewise, Trz brings a smaller increase of EA_X (0.36 eV), but much bigger increase of EA_M (1.36 eV), thus leading to a significantly increased $BDE_f(-)$ (2.42 eV) for **C4**. Intriguingly, $BDE_f(-)$ values of the 2-site-substituted isomers are 1.78, 2.15, and 2.62 eV for **C5**, **C6**, and **C7**, respectively; which are 0.2−0.4 eV higher than those of 3-site-substituted isomers. That is because the substituent at 2-site has a stronger interaction with the LUMO of Cz, but a relatively weaker interaction with the SUMO of Cz radical (Supplementary Fig. S9). Notably, although 3,6-substitutions are widely used in Cz-derivatives, the result here shows that 2,7-substitutions has greater advantage on improving the intrinsic molecular stability. In principle, substitutions on C-side of PhCz-derivatives solely increase EA_M, thus have advantage for increasing $BDE_f(-)$. As shown in Fig. 4b, cyano and 4,6-diphenyl-1,3,5-triazin-2-yl on the phenyl of **C8** and **C9** significantly increases their $BDE_f(-)$ to 2.26 and 3.02 eV, which are much higher than those of the N-side-substituted counterparts.

Improving $BDE_f(-)$ values of donor (D)−π−acceptor (A) molecules

Most OLED molecules have D−π−A structures, in which the fragile bonds are either in D, A or in both. To explore the distinct effects of substituted position in D−π−A molecules, we designed a group of molecules based on (3-(9H-carbazol-9-yl)phenyl)diphenylphosphineoxide (CzPO, Fig. 4c), with Cz and PO as D and A, respectively. Its C−P and C−N bonds have comparable BDE(−) values (1.90 *vs* 2.00 eV). The typical D-EWG Trz is introduced to the 2-site of Cz (**D-Trz**), *para*-position of $POPh_2$ (**A-Trz**), or on the central phenyl (**π-Trz**). $BDE_f(-)$ values in **D-Trz**, **A-Trz**, and **π-Trz** are 2.80, 2.89, and 3.08 eV for C−P bonds; and 2.67, 3.26, and 3.20 eV for C−N bonds, respectively (Fig. 4d). These values are 0.67−1.26 eV higher than those of CzPO. Compared with D- or A-substituted counterparts, **π-Trz** clearly reinforces all the fragile bonds from donor and acceptor. The framework not only makes each group contribute to EA_M, but also keeps them being spatially separated, preventing them from increasing EA_X (the details are in Supplementary Fig. S10). Therefore, employing D-EWGs at the π-side (*center*) of the molecule is most recommended for developing robust D−π−A molecules.

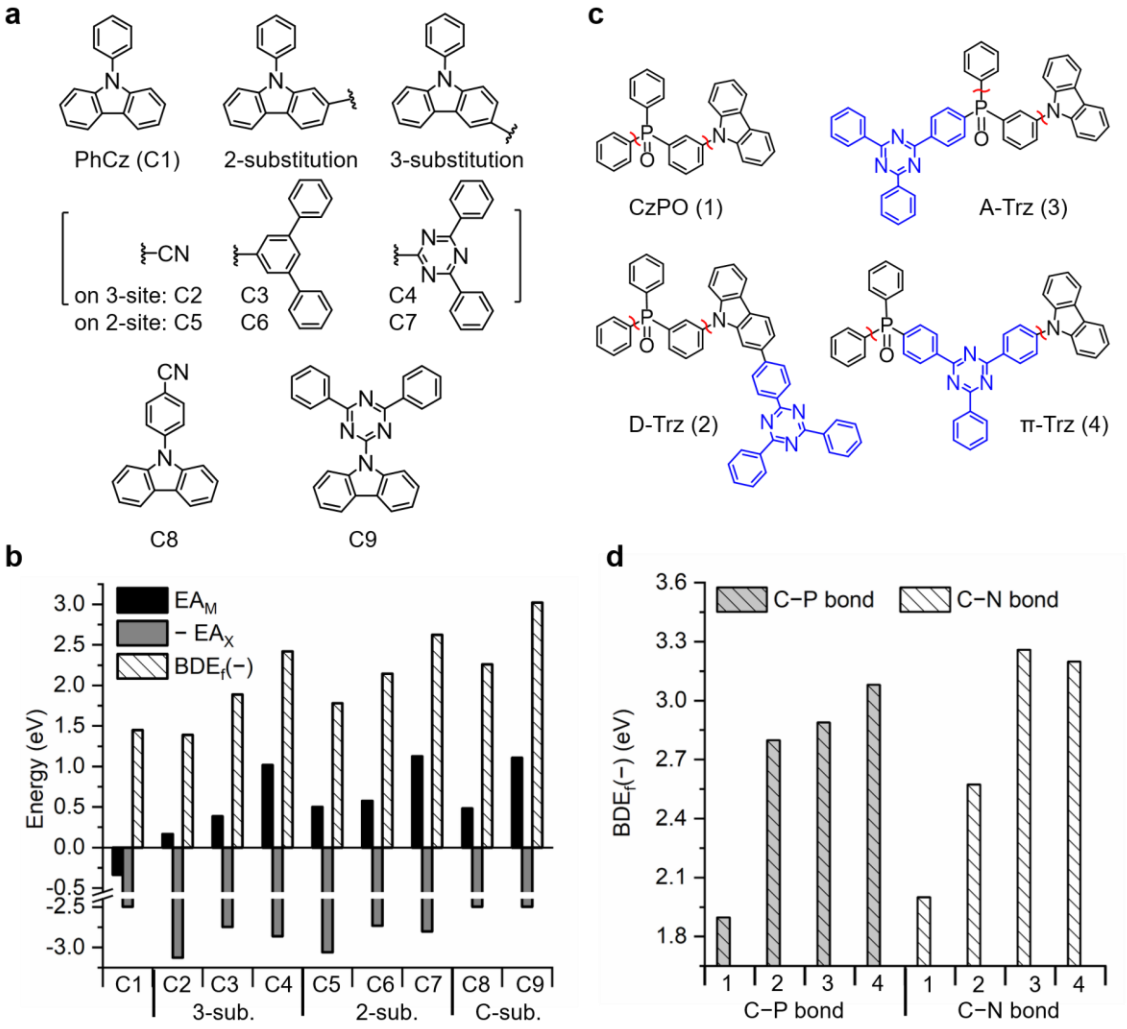

Figure 4 | Study on improving $BDE_f(-)$ values of Cz-derivatives and D−π−A molecules. a, Chemical structures of PhCz and its derivatives, $BDE_f(-)$ values of the fragile C−N bonds were calculated. **b,** EA_M, EA_x, and $BDE_f(-)$ values of PhCz-derivatives **C1**−**C9**. **c,** Chemical structures of CzPO-derivatives with D−π−A backbones. The fragile C−N and C−P bonds are highlighted by the red markers. **d,** $BDE_f(-)$ values of the fragile bonds of CzPO-derivatives. All calculations were at the M06-2X/def2-SVP level.

Implications for rational design of robust OLED materials

In OLED molecules, many building blocks can contribute to desirable optical/electrical performance. PO is a representative instance, which often plays an important role in the corresponding high-efficiency materials.[38–43] Unfortunately, when PO is the sole acceptor, the corresponding molecules often suffer from low $BDE_f(-)$ values and poor material stability, as clearly demonstrated by CzPO2 and TP3PO. Similar issues may occur to other typical blocks like biphenyl, triphenylsilyl, or a single azine ring, which are evidenced by the low $BDE_f(-)$ values of **A1**−**A3** (1.48−2.33 eV, Fig. 5a and 5b). To enhance the molecular stability towards electrons, exclusively using strong and stable acceptors is indeed viable. The Trz, cyano, and carbonyl undoubtedly guarantee high $BDE_f(-)$ values (2.81−3.33 eV for **B4**−**B6**, Fig. 5c). Nevertheless, abundant building blocks are always desired to meet the various needs in practical applications.

Here, we propose a superior approach by introducing or constructing D-EWGs to revive the building blocks that may lead to low $BDE_f(-)$ values. The effectiveness can be evidenced by the reported **C1**−**C4**, which retain the blocks and fragile bonds in **A1**−**A4**, but combine them with extra strong EWGs, constructing D-EWGs at the center of the molecule. Markedly different

from **A1**−**A4**, **C1**−**C4** have substantially improved $BDE_f(-)$ values (2.55−3.17 eV, Fig. 5b), clearly manifesting that the preservation of these blocks would not sacrifice the molecular stability. Meanwhile, these groups like PO could bring desirable optical and electrical performance, as evidenced by **C4** with a tenfold increase of radiation rate constant and a fivefold decrease of non-radiation rate constants compared with PO-free counterparts.[41] The improved molecular stability of **C1**−**C4** can be evidenced by the reported experiments. Lee *et al.* found that **C1**-based EOD are robust towards electrons.[45] Kwon *et al.* replaced **A1** with **C1** as the host of a blue-OLED based on the consideration of BDE(−), which gave a ~7 fold increase of device lifetime.[46] Duan *et al.* found the **C2**-based OLED have a substantially prolonged lifetime compared with that based on **A2**,[47] in which the significantly increased $BDE_f(-)$ should not be neglected. **C3** is reported as a robust host even for pure blue phosphorescent OLEDs.[48] The superior molecular stability of **C4** to **A4** has been demonstrated above.

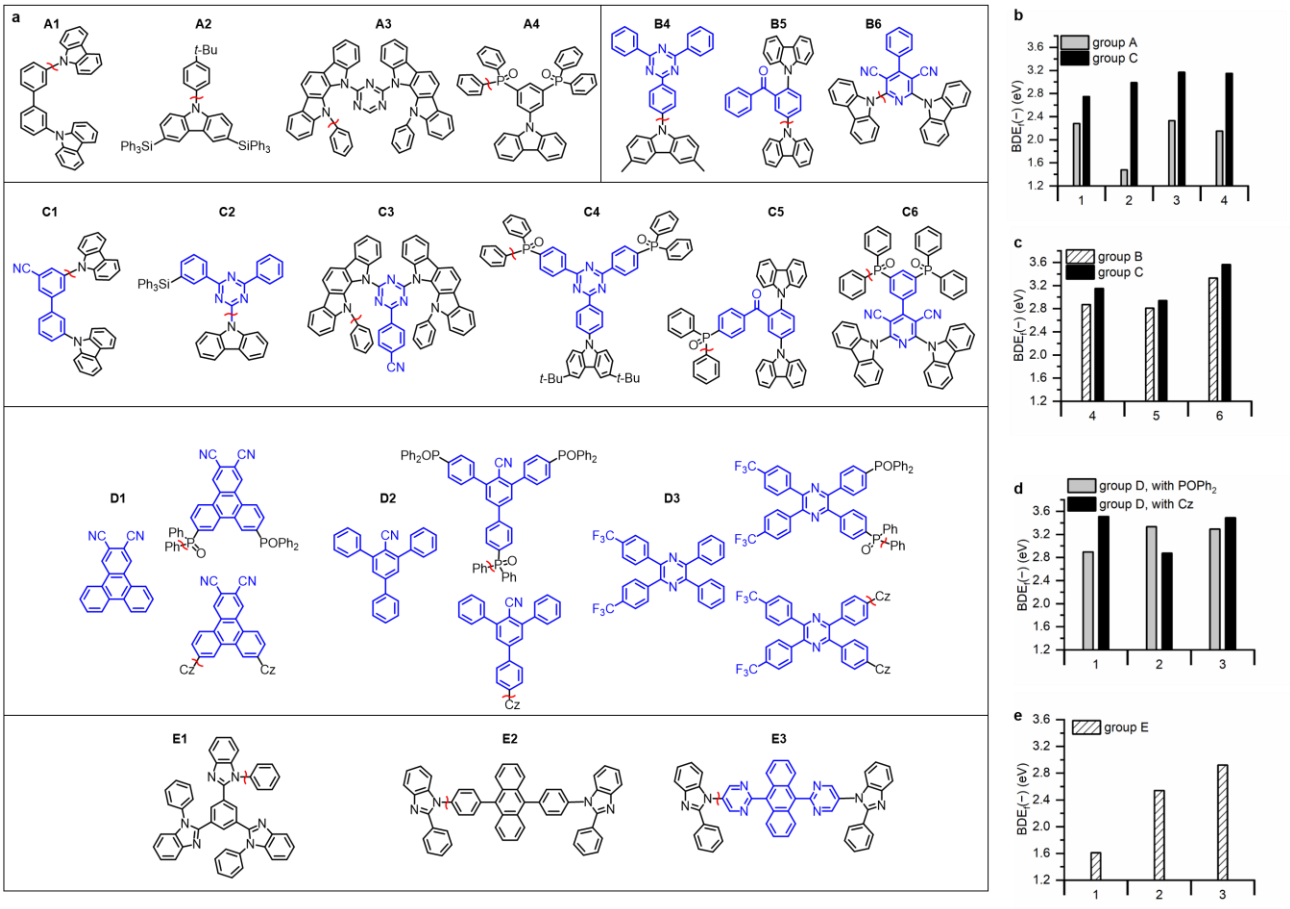

Figure 5 | Instances of improved $BDE_f(-)$ values by D-EWGs. a, Chemical structures of reported or newly designed OLED molecules. Their fragile bonds are highlighted by the red markers. **b−e,** $BDE_f(-)$ values of the molecules in: group A and C (**b**); group B and C (**c**); group D (**d**); and group E (**e**). Among which, molecule **C5**, **C6**, **E3**, and all of the molecules in group D are newly designed in this work. The D-EWG moieties are highlighted in blue color. All calculations were at the M06-2X/def2-SVP level.

Previously, we suggested that PO groups would undermine the molecular stability due to the low BDE_f of C−P bonds. Presently, it is reasonable to deduce that for molecules already with D-EWGs, introducing groups PO will be benign to their molecular stabilities. The comparison between the $BDE_f(-)$ values of **C4** and **B4** (3.15 vs 2.87 eV) gives a good instance. We further designed **C5** and **C6** with PO groups combined with benzophenone and cyanopyridine, respectively. Calculations show that they have even higher $BDE_f(-)$ values (2.94 and 3.56 eV) than those of **B2** and **B3** (2.81 and 3.33 eV). Therefore, introducing D-EWGs is very effective and viable to revive the original vulnerable building blocks for the development of

robust OLED materials.

To enrich the building blocks for robust OLED materials, we designed three new blocks **D1**−**D3** (Fig. 5a) with D-EWG substructures. We expect they can stabilize various fragile bonds from electrons, and thus allowing high tunability for molecular design. Indeed, whether combined with PO or Cz, the corresponding molecules all show high $BDE_f(-)$ values (2.87−3.55 eV, Fig. 5d). Finally, we show that the strategy is also effective for systems other than Cz/PO. For ETMs based on benzimidazole-derivatives, the classic TPBi (**E1**) has particularly low $BDE_f(-)$ (1.61 eV, Fig. 5e) for the C−N bond. In comparison, **E2** with extended π-conjugation has a higher $BDE_f(-)$ (2.54 eV). Notably, compared with **E1**-based counterparts, **E2**-based OLEDs have a ∼3 fold increase of device lifetime,[49] in which the improved $BDE_f(-)$ should have a non-negligible contribution, although the authors did not mentioned. Based on **E2**, we constructed 9,10-di(pyrimidin-2-yl)anthracene as a D-EWG, which further improves $BDE_f(-)$ to 2.92 eV for **E3**. It is certain that the newly designed **E3** with substantially higher $BDE_f(-)$ would be even more robust towards electrons. Overall, these examples further consolidate that our strategy would be universal and effective for improving the molecular stability of OLED materials.

Conclusions

In this work, we first emphasized $BDE_f(-)$ is a little-watched molecular parameter but of vital importance for organic (opto)electronic materials, and revealed the close correlation between $BDE_f(-)$, materials stability, and device lifetime. The comparative study on typical ETMs TP3PO and PO-T2T clearly demonstrated that active organic materials with lower $BDE_f(-)$ do result in poorer materials stability and device lifetime. We then explored how to manipulate $BDE_f(-)$. Based on the Hess's law, regulating $BDE_f(-)$ is converted to the explicit modulations of EA_M and EA_X. We found that introducing D-EWGs can significantly improve EA_M, but has much smaller effect on EA_X, thus substantially improving the $BDE_f(-)$ (∼1 eV) for various OLED materials. Meanwhile, the bond cleavage process will be hindered by such D-EWGs due to their strong confinement of the negative charge. The effectiveness and generality of this strategy has been validated by the comparisons in several groups of reported and newly designed molecules. Importantly, it can make the original vulnerable group no longer vulnerable towards electrons, thus largely enriching available building blocks for the design of robust OLED materials. Also, the strategy would be transferrable to other organic (opto)electronic materials. At the end, it should be noted that this research looked into the manipulations of BDE(−) of C−X bonds, which helps to deepen the understanding on the relationship between molecular structures and BDE(−) values for all organic compounds. Since chemistry is mainly based on the bond reorganization process, the study on BDE could be beneficial for various researches in chemistry and material sciences.

Acknowledgements

This work was supported by the National Key R&D Program of China (No. 2016YFB0401003, 2016YFB0400702) and the National Science Fund of China (Grant Nos. 51525304) for financial support. We are grateful to Prof. Hui Xu *et al.* and Prof. Qisheng Zhang *et al.* for providing the sample of *p*tBCzPO2TPTZ and TCzTrz, respectively. We are also grateful to the High-Performance Computing Center in Tsinghua University and Tsinghua Xuetang Talents Program for supporting the computational resources.

Author contributions

R.W. and J.Q. wrote the manuscript with the aid of Q.-Y.M. and Y.-L.W. R.W. performed the theoretical calculations with the aid of Q.-Y.M. and Y.-L.W. R.W. and Q.-Y.M performed the LDI-TOF-MS test, EOD and OLED fabrications and measurements. Y.-L.W. and J.Q. analyzed the calculation and experimental results and guided R.W. for calculation planning

and data interpretation. J.Q. supervised the entire research. All authors discussed the progress of the research and reviewed the manuscript.

Additional information

Supplementary information is available in the online version of the paper. Reprints and permissions information is available online at www.nature.com/reprints. Correspondence and requests for materials should be addressed to J.Q.

Competing interests

The authors declare no competing interests.

REFERENCES

1. Ostroverkhova, O. Organic optoelectronic materials: mechanisms and applications. *Chem. Rev.* **116**, 13279–13412 (2016).
2. Mateker, W. R. & McGee, M. D. Progress in understanding degradation mechanisms and improving stability in organic photovoltaics. *Adv. Mater.* **29**, 1603940 (2017).
3. Quinn, J. T. E., Zhu, J., Li, X., Wang, J. & Li, Y. Recent progress in the development of n-type organic semiconductors for organic field effect transistors. *J. Mater. Chem. C*, **5**, 8654-8681 (2017).
4. Scholz, S., Kondakov, D., Lüssem, B. & Leo, K. Degradation mechanisms and reactions in organic light-emitting devices. *Chem. Rev.* **115**, 8449–8503 (2015).
5. Zhao, C. & Duan, L. Review on photo- and electrical aging mechanisms for neutral excitons and ions in organic light-emitting diodes. *J. Mater. Chem. C* **8**, 803-820 (2020).
6. Song, W. & Lee, J. Y. Degradation mechanism and lifetime improvement strategy for blue phosphorescent organic light-emitting diodes. *Adv. Opt. Mater.* **5**, 1600901 (2017).
7. Schmidbauer, S., Hohenleutner, A. & Konig, B. Chemical degradation in organic light-emitting devices: mechanisms and implications for the design of new materials. *Adv. Mater.* **25**, 2114-2129 (2013).
8. Jeon, S. K., Lee, H. L., Yook, K. S. & Lee, J. Y. Recent Progress of the Lifetime of Organic Light-Emitting Diodes Based on Thermally Activated Delayed Fluorescent Material. *Adv. Mater.* **31**, e1803524 (2019).
9. Cai, X. & Su, S.-J. Marching toward highly efficient, pure-blue, and stable thermally activated delayed fluorescent organic light-emitting diodes. *Adv. Funct. Mater.* **28**, 1802558 (2018).
10. Giebink, N.C. *et al.* Intrinsic luminance loss in phosphorescent small-molecule organic light emitting devices due to bimolecular annihilation reactions. *J. Appl. Phys.* **103** (2008).
11. Zhang, Y., Lee, J. & Forrest, S.R. Tenfold increase in the lifetime of blue phosphorescent organic light-emitting diodes. *Nat. Commun.* **5**, 5008 (2014).
12. Song, W., Lee, J.Y., Kim, T., Lee, Y. & Jeong, H. Comprehensive understanding of degradation mechanism of high efficiency blue organic light-emitting diodes at the interface by hole and electron transport layer. *Org. Electron.***57**, 158-164 (2018).
13. Sohn, J. *et al.* Degradation mechanism of blue thermally activated delayed fluorescent organic light-emitting diodes under electrical stress. *Org. Electron.* **70**, 286-291 (2019).
14. Tanaka, M., Nagata, R., Nakanotani, H. & Adachi, C. Understanding degradation of organic light-emitting diodes from magnetic field effects. *Commun. Mater.* **1** (2020).
15. Shao, M., Yan, L., Li, M., Ilia, I. & Hu, B. Triplet–charge annihilation versus triplet–triplet annihilation in organic semiconductors. *J. Mater. Chem. C* **1**, 1330-1336 (2013).
16. Xu, H., Wang, M., Yu, Z.-G., Wang, K. & Hu, B. Magnetic field effects on excited states, charge transport, and electrical polarization in organic semiconductors in spin and orbital regimes. *Adv. Phys.* **68**, 49-121 (2019).
17. Lee, J. *et al.* Hot excited state management for long-lived blue phosphorescent organic light-emitting diodes. *Nat. Commun.* **8**, 15566 (2017).
18. Ha, D. G. *et al.* Dominance of exciton lifetime in the stability of phosphorescent dyes. *Adv. Opt. Mater.* **7**, 1901048 (2019).
19. Noda, H., Nakanotani, H. & Adachi, C. Excited state engineering for efficient reverse intersystem crossing. *Sci. Adv.*, **4**, eaao6910 (**2018**).
20. Han, S.H., Jeong, J.H., Yoo, J.W. & Lee, J.Y. Ideal blue thermally activated delayed fluorescence emission assisted by a thermally activated delayed fluorescence assistant dopant through a fast reverse intersystem crossing mediated cascade energy transfer process. *J. Mater. Chem. C* **7**, 3082-3089 (2019).

21. Zhang, D., Cai, M., Zhang, Y., Zhang, D. & Duan, L. Sterically shielded blue thermally activated delayed fluorescence emitters with improved efficiency and stability. *Mater. Horiz.* **3**, 145-151 (2016).
22. Ligthart, A. *et al*. Effect of triplet confinement on triplet–triplet annihilation in organic phosphorescent host–guest systems. *Adv. Funct. Mater*. **28**, 1804618 (2018).
23. Bangsund, J. S., Hershey, K. W. & Holmes, R. J. Isolating degradation mechanisms in mixed emissive layer organic light-emitting devices. *ACS Appl. Mater. Interfaces* **10**, 5693-5699 (2018).
24. Jeong, C. *et al.* Understanding molecular fragmentation in blue phosphorescent organic light-emitting devices. *Org. Electron.* **64**, 15-21 (2019).
25. Freidzon, A.Y. *et al.* Predicting the operational stability of phosphorescent OLED host molecules from first principles: a case study. *J. Phys.Chem. C* **121**, 22422-22433 (2017).
26. Wang, R. *et al.* Effects of ortho-linkages on the molecular stability of organic light-emitting diode materials. *Chem. Mater*. **30**, 8771-8781 (2018).
27. Lin, N. *et al.* Achilles heels of phosphine oxide materials for OLEDs: chemical stability and degradation mechanism of a bipolar phosphine oxide/carbazole hybrid host material. *J. Phys. Chem. C* **116**, 19451-19457 (2012).
28. Lin, N., Qiao, J., Duan, L., Wang, L. & Qiu, Y. Molecular understanding of the chemical stability of organic materials for OLEDs: a comparative study on sulfonyl, phosphine-oxide, and carbonyl-containing host materials. *J. Phys. Chem. C* **118**, 7569-7578 (2014).
29. Kondakov, D.Y. Role of chemical reactions of arylamine hole transport materials in operational degradation of organic light-emitting diodes. *Journal of Applied Physics* **104**, 084520 (2008).
30. Kondakov, D. Y., Lenhart, W. C. & Nichols, W. F. Operational degradation of organic light-emitting diodes: Mechanism and identification of chemical products. *J. Appl. Phys.* **101**, 024512 (2007).
31. Scholz, S., Walzer, K. & Leo, K. Analysis of complete organic semiconductor devices by laser desorption/ionization time-of-flight mass spectrometry. *Adv. Funct. Mater.* **18**, 2541-2547 (2008).
32. Sandanayaka, A.S.D., Matsushima, T. & Adachi, C. Degradation mechanisms of organic light-emitting diodes based on thermally activated delayed fluorescence molecules. *J. Phys. Chem. C* **119**, 23845-23851 (2015).
33. Byeon, S.Y., Han, S.H. & Lee, J.Y. Negative polaron-stabilizing host for improved operational lifetime in blue phosphorescent organic light-emitting diodes. *Adv. Opt. Mater.* **5** (2017).
34. Hong, M., Ravva, M.K., Winget, P. & Brédas, J.-L. Effect of substituents on the electronic structure and degradation process in carbazole derivatives for blue OLED host materials. *Chem. Mater.* **28**, 5791-5798 (2016).
35. Cheng, J. P., & Zheng, Z. Carbon-halogen bond cleavage energies of polyhaloalkyl radical anions in solution. *Tetra. lett*. **37**, 1457-1460 (1996).
36. Houmam, A. Electron Transfer initiated reactions: bond formation and bond dissociation. *Chem. Rev.* **108,** 2180–2237 (2008).
37. Daasbjerg, K. Estimation of bond dissociation Gibbs energies for carbon-halogen bonds in anion radicals of some aryl halides and substituted benzyl halides. *J. Chem. Soc. Perkin Trans.* **2,** 1275-1277 (1994).
38. Schaub, T.A. *et al.* A Stable crystalline triarylphosphine oxide radical anion. *Angew Chem Int Ed* **55**, 13597-13601 (2016).
39. Yang, H., Liang, Q., Han, C., Zhang, J. & Xu, H. A phosphanthrene oxide host with close sphere packing for ultralow-voltage-driven efficient blue thermally activated delayed fluorescence diodes. *Adv. Mater.* **29,** 1700553 (2017).
40. Lee, S. Y., Adachi, C. & Yasuda, T. High-Efficiency blue organic light-emitting diodes based on thermally activated delayed fluorescence from phenoxaphosphine and phenoxathiin derivatives. *Adv. Mater.* **28,** 4626-4631 (2016).
41. Li, C., Duan, C., Han, C. & Xu, H. Secondary acceptor optimization for full-exciton radiation: toward sky-blue thermally activated delayed fluorescence diodes with external quantum efficiency of ≈30%. *Adv. Mater.* **30,** 1804228 (2018).
42. Gong, S., Chang, Y.-L., Wu, K., White, R., Lu, Z.-H., Song, D. & Yang, C. High-power-efficiency blue electrophosphorescence enabled by the synergistic combination of phosphine-oxide-based host and electron-transporting materials. *Chem. Mater.* **26,** 1463-1470 (2014).
43. Jia, J., Zhu, L., Wei, Y., Wu, Z., Xu, H., Ding, D., Chen, R., Ma, D. & Huang, W. Triazine-phosphine oxide electron transporter for ultralow-voltage-driven sky blue PHOLEDs. *J. Mater. Chem. C* **3,** 4890-4902 (2015).
44. Liu, Z. *et al.* A high fluorescence rate is key for stable blue organic light-emitting diodes. *J. Mater. Chem. C* **6**, 7728-7733 (2018).
45. Ihn, S.-G., Lee, N., Jeon, S. O., Sim, M., Kang, H., Jung, Y., Huh, D. H., Song, Y. M., Lee, S. Y., Numata, M., Miyazaki, H., Gómez-Bombarelli, R., Aguilera-Iparraguirre, J., Hirzel, T., Aspuru-Guzik, A., Kim, S. & Lee, S. An alternative host material for long-lifespan blue organic light-emitting diodes using thermally activated delayed fluorescence. *Adv. Sci.* **4,** 1600502 (2017).

46. Ahn, D. H., Maneg, J. H., Lee, H., Yoo, H., Lampande, R., Lee, J. Y. & Kwon, J. H. Rigid oxygen-bridged boron-based blue thermally activated delayed fluorescence emitter for organic light-emitting diode: approach towards satisfying high efficiency and long lifetime together. *Adv. Optical Mate*r. **8,** 2000102 (2020).
47. W. Liu, C. J. Zheng, K. Wang, Z. Chen, D. Y. Chen, F. Li, X. M. Ou, Y. P. Dong & X. H. Zhang. Novel carbazol-pyridine-carbonitrile derivative as excellent blue thermally activated delayed fluorescence emitter for highly efficient organic light-emitting devices. *ACS Appl. Mater. Interfaces* **7,** 18930-18936 (2015).
48. Jung, M., Lee, M. H., Lee, H. Y. & Kim, T. A bipolar host based high triplet energy electroplex for an over 10,000 h lifetime in pure blue phosphorescent organic light-emitting diodes. *Mater. Horiz.* **7,** 559-565 (2020).
49. Zhang, D., Wei, P., Zhang, D. & Duan, L. Sterically shielded electron transporting material with nearly 100% internal quantum efficiency and long lifetime for thermally activated delayed fluorescent and phosphorescent OLEDs. *ACS Appl. Mater. Interface* **9,** 19040−19047 (2017).

Methods

LDI-TOF-MS Measurement. The samples of TP3PO and PO-T2T were purchased from commercial resources, and had been sublimed to guarantee the purity. The measurement was performed with a Shimadzu AXIMA Performance MALDI-TOF instrument under the negative detection mode. The applied voltage between the target and the TOF aperture is 25 kV. The samples were excited by the pulsed nitrogen laser (337 nm). The maximum pulsed laser power is 180 μJ/pulse (at 50 Hz). The sample powder was dissolved by chromatogram class acetone or dichloromethane without assistant matrix. After solvent evaporation, the thin film was excited by the laser beam with different power intensity.

Device Fabrication and Test. For all devices, the ITO-coated glass substrates were precleared and treated by UV-ozone for 30 minutes. The evaporation processes were performed at a pressure under 1×10^{-4} Pa. The deposition rate for organic materials, LiF, and Al were 0.1 nm/s, 0.01 nm/s, and 0.3 nm/s, respectively. Chemical structures of the involved materials in electron-only devices and OLED devices are in Supplementary Fig. S5. All of the materials were purchased from commercial resources. The forward-viewing electronic characteristics of the devices were measured by a Keithley 2400 source meter. The EL characteristics of the devices were obtained on a PR650 spectrometer.

Computational Details. Calculations and analysis in this work were performed with Gaussian 09 (D.01) and Multiwfn (3.7).[50,51] BDE and EA values were calculated as the enthalpy changes of the bond cleavage and electron attachment reactions at 298.15K and 1 atm (gas phase), respectively. The corresponding geometry optimizations and frequency analysis were performed at the density functional theory (DFT) level using M06-2X functional and def2-SVP basis set. The functional is known to be good at calculating main-group thermochemistry.[52] The rationality of using diffusion function-free basis set to study the variations of BDE(−) and EA values of OLED molecules are previously demonstrated by Brédas *et al.*[34] We also confirmed that the BDE_f(−) and EA values calculated through def2-SVP basis set retain the same trends as those calculated via the double-ζ basis set with diffuse functions 6-31+G(d,p) (Supplementary Fig. S11), while the former basis set is more cost effective. In addition, we compared the BDE values derived from M06-2X/def2-SVP, the common B3LYP/6-31G* and the benchmark Complete Basis Set-Quadratic Becke3 (CBS-QB3) method, the detailed data are shown in Supplementary Table S7.

In additions to the BDEs, other molecular parameters were calculated to help understand the correlations between the BDEs and molecular structures. Spin density distribution (SDD) is defined as the differences between the α and the β electron densities of each point in the space. In negatively charged species, the amount of negative charge allocated on a certain group R (q_R) is calculated by the following equation (2).

$$q_R = \sum_{i \in R}(q_i^{neg} - q_i^{neu}) \quad (2)$$

Here, i includes each atom in group R; q_i^{neu} and q_i^{neg} are the Hirshfeld charges of i in the neutral and negatively charged states of the corresponding structure, respectively.

REFERENCES

50. Frisch, M. J. *et al.* Gaussian 09, revision D.01; Gaussian, Inc.: Wallingford, CT (2009).
51. Lu, T. & Chen, F. Multiwfn: A multifunctional wavefunction analyzer. *J. Comput. Chem.* **33**, 580-592 (2012).
52. Narbe, M. & Head-Gordon, M. Thirty years of density functional theory in computational chemistry: an overview and extensive assessment of 200 density functionals. *Mol. Phys.* **115**, 2315-2372 (2017).